Role of lipid rafts in Shiga toxin 1 interaction with the apical surface of Caco-2 cells

Olga Kovbasnjuk[1,*], Michael Edidin[2] and Mark Donowitz[1]

[1]Department of Medicine, Johns Hopkins University, Baltimore, MD, USA
[2]Department of Biology, Johns Hopkins University, Baltimore, MD, USA
*Author for correspondence (e-mail: olukrn@yahoo.com)

Accepted 8 August 2001
Journal of Cell Science 114, 4025-4031 (2001) © The Company of Biologists Ltd

SUMMARY

Enterohemorrhagic *Escherichia coli* producing Shiga toxins 1 and/or 2 have become major foodborne pathogens. The specific binding of Shiga toxin 1 B-subunit to its receptor, a neutral glycolipid globotriaosylceramide Gb_3, on the apical surface of colonic epithelium followed by toxin entry into cells are the initial steps of the process, which can result in toxin transcytosis and systemic effects of infection including hemolytic uremic syndrome. Understanding the complex mechanisms of Shiga toxin 1 binding and internalization may help to develop new strategies directed at preventing toxin internalization. Fluorescence resonance energy transfer microscopy revealed the clustering of Shiga toxin receptors Gb_3 in lipid rafts with another glycosphingolipid G_{M1} on the apical surface of highly polarized intestinal epithelial Caco-2 cells. Lipid rafts disruption significantly decreased internalization of Shiga toxin 1 B-subunit. Although disruption of lipid rafts by cholesterol depletion did not affect the amount of bound Shiga toxin 1 B-subunit, lipid rafts are necessary for toxin uptake across the apical membrane of Caco-2 cells.

Key words: Shiga toxin, Globotriaosylceramide Gb_3, Lipid rafts, Cholesterol, Caco-2 cells

INTRODUCTION

Enterohemorrhagic *Escherichia coli* (EHEC) are responsible for life-threatening foodborne illnesses consisting of diarrhea and the hemolytic uremic syndrome (HUS) (Acheson, 1999), and are the leading cause of acute renal failure in children in the USA, with a mortality of 5-10% (Robson et al., 1991). EHEC have a variety of transmission pathways including contaminated food and water, infected individuals and even the house fly (Acheson, 1999). Moreover, there is no effective therapy for this illness, and antibiotic treatment of children with this infection increases the risk of HUS (Wong et al., 2000).

A major mechanism for the serious complications of EHEC infection involves production of Shiga toxins (Stx) 1 and 2 by bacteria. Stx are members of the so-called AB_5 class of bacterial toxins. Stx consist of hexameric assemblies comprising a single catalytically active A-subunit and a pentamer of identical B-subunits, which are responsible for toxin attachment to the host cells (Lacy and Stevens, 1998). The receptor for Stx is the neutral glycolipid Gb_3 with terminal sugar residues αGal(1-4)βGalβGlc-ceramide (Lindberg et al., 1987). Even in the absence of A subunit, the B subunits still form pentamers that are functionally equivalent to the holotoxin in binding to cell surface glycolipids (Jacewicz et al., 1986). The crystal structure of Stx1 B-pentamer (Stx1B) complexed with a Gb_3 analogue revealed the existence of three Gb_3-binding sites per B-subunit (Ling et al., 1998). Two of the binding sites are constructed by residues from two different monomers and thus require the pentameric assembly of the B-subunit. The binding constant of Stx to whole cells is 10^9 M^{-1} (Fuchs et al., 1986); however, the binding constant to soluble Gb_3 is only about 10^3 M^{-1} (St Hilaire et al., 1994). The toxin circumvents the low affinity by binding simultaneously to five or more cell surface carbohydrates.

Stx1B binding to a terminal sugar residue of Gb_3 is the initial step in a cascade leading to epithelial and endothelial cell damage. The importance of the B-pentamer-Gb_3 interaction is illustrated by the fact that all cells that are susceptible to Stx1 express Gb_3 on their cell surfaces, whereas cells such as CHO and T84 that do not express Gb_3 are resistant to the toxin (Jacewicz et al., 1994; Acheson et al., 1996). In addition, in vivo toxicity is correlated with binding affinity (Weinstein et al., 1989). Understanding the complex mechanism of Stx1 binding to the apical membrane and internalization into colonic epithelial cells, the earliest steps of intoxification, may help in the development of strategies to prevent toxin internalization and translocation across the intestinal epithelia.

It was shown recently (Katagiri et al., 1999) that the majority of plasma membrane Gb_3 resides in detergent insoluble microdomains (DIM), also known as lipid rafts (LR). We hypothesized that the high local concentration of receptor molecules and their clustering in rafts could play an important role in the initial binding of Stx1B and the subsequent toxin transfer across the membrane. However, the actual existence of LR in living cell membranes has been a matter of debate (Jacobson and Dietrich, 1999; Kenworthy et al., 2000), and there is even evidence that molecular clustering is caused by detergent treatment of the plasma membrane (Mayor and Maxfield, 1995).

The aim of this study was to test whether Gb_3 molecules are in LR in plasma membrane of living polarized Caco-2 cells.

These cells when differentiated represent a model of upper crypt/lower villus cells of the small intestine – a natural target of Stx1 in the intestine (Acheson et al., 1991). Hence, we also aimed to see if the clustering of Gb_3 molecules plays an essential role in Stx1B interaction with the apical surface of intestinal epithelial cells. Here we show, using fluorescence resonance energy transfer (FRET), that Gb_3 receptors are clustered in native plasma membranes with the LR marker G_{M1} (Abrami and van der Goot, 1999). Our data demonstrate that depleting cholesterol, which disrupts LR, abolishes FRET between Gb_3 and G_{M1}, but does not influence Stx1B binding. However, cholesterol depletion has a profound effect on Stx1B transfer across the apical membrane of Caco-2 cells. Based on these data, we propose that Gb_3-rich membrane microdomains, in addition to Stx1B receptors, contain other elements that are involved in toxin uptake, and that the microdomains are necessary for the transfer of bound toxin into the cell and subsequent cell intoxification.

MATERIALS AND METHODS

Materials

Purified Stx1B labeled with Cy5 fluorescent dye was the generous gift of D. W. K. Acheson (New England Medical Center, Boston, MA). Purified cholera toxin B-subunit (CTB) and CTB conjugated with tetramethylrhodamine (TMR) fluorescent dye were from List Biological Laboratories Inc. (Campbell, CA). Filipin, cholesterol oxidase and methyl-β-cyclodextrin (MβCD) were obtained from Sigma. Oregon Green 488 fluorescent dye, TMR-labeled 10K dextran and Alexa 594-conjugated albumin were from Molecular Probes (Eugene, OR).

Cell culture

Caco-2 cells derived from human colonic adenocarcinoma were cultured in DMEM containing 26 mM $NaHCO_3$ supplemented with 0.1 mM non-essential amino-acids, 10% FBS, glutamine, 50 U/ml penicillin, 50 μg/ml streptomycin, pH 7.4 in 5% CO_2 atmosphere at 37°C. For experimental purposes the cells were grown to confluence on glass coverslips and were used between 10-15 days after reaching confluence.

Fluorescent toxin preparation

In experiments measuring FRET, bisfuntional succimidyl ester derivatives of the cyanine dyes Cy3 and Cy5 (Amersham Life Science Inc., Arlington Heights, IL) were conjugated to purified CTB and Stx1B, respectively, according to the manufacturer's instructions. The conjugation reaction was stopped by passage over a column (10DG column, BioRad Laboratories, Hercules, CA) to separate the conjugated proteins from the unbound dyes.

In experiments measuring CTB and Stx1B co-localization and Stx1B binding and/or internalization, the purified B-subunit of Stx1 was labeled with Oregon Green 488 (OrG488) fluorescent dye (Molecular Probes, Eugene, OR) according to the manufacturer's instructions.

Co-localization analysis

Confocal 8-bit images of Caco-2 cell surface labeled with TMR-CTB (red) and OrG488-Stx1B (green) were generated using a multiphoton laser scanning imaging system (MRC-1024 MP, Biorad, Hercules, CA) based on an upright E600FN Nikon microscope (Japan), which is connected to a mode-locked Ti:sapphire laser (Tsunami, Spectra-Physics, Mountain View, CA). The marker fluorescence was visualized using a water immersion 60×/1.2 Plan Apo objective lens (Nikon). Pixel intensity levels were adjusted in the linear range of detectors by LaserSharp 3.2 software (Biorad) before images were taken so that maximum and minimum values were between 0 and 255 gray levels (GL) in each photomultiplier channel.

For quantitation of overlap between two fluorescent toxins, pairs of images (green and red) were equally inclusively thresholded using MetaMorph (Universal Imaging, Downingtown, PA) to exclude background fluorescence and cells that did not express CTB and Stx1B receptors from analysis. The resulting images represent only pixels, which are positive for the markers. The amount of Stx1B-positive pixels that overlap with CTB positive pixels was calculated by the MetaMorph Measure Co-localization function for each chosen cell and expressed as a percentage.

Immunofluorescence labeling

In experiments measuring FRET, Caco-2 cells grown on glass coverslips were labeled for 30 minutes with a mixture of donor (Cy3)- and acceptor (Cy5)-labeled toxins diluted in PBS buffer, pH 7.4 at 4°C to prevent endocytosis. Cells were washed twice with cold PBS and then fixed for 1 hour in 3% paraformaldehyde in PBS. Finally, the coverslips were washed three times in PBS, mounted on slides and sealed with nail polish. The concentration of donor Cy3-conjugated CTB was held constant in each mixture, and Cy5-conjugated Stx1B was added to give the indicated ratio of donor to acceptor (D:A)=1:3 (2:6 μg/ml) or 1:1 (2:2 μg/ml).

In experiments measuring Stx1B binding and internalization, monolayers were incubated with Stx1B-OrG488 at 37°C for 30 minutes, then free fluorescent toxin was washed away, and monolayers were mounted on glass slides or in a spectrofluorometer chamber for quantitation of fluorescence intensity. In experiments measuring the Stx1B binding, cells were stained with Stx1B-OrG488 at 4°C for 30 minutes, fixed for 1 hour in 3% paraformaldehyde and mounted on glass slides or in a spectrofluorometer chamber for fluorescence intensity quantitation.

In both types of experiments, LR were disrupted by incubation of cells with 1 μg/ml filipin for 20 minutes, 100 mg/ml mβCD or 0.5 U/ml cholesterol oxidase for 1 hour at 37°C. Then monolayers were washed with PBS and labeled and fixed as above.

In experiments to measure dextran (M_r 10×10^3) or albumin (both 10 μg/ml) internalization, control and MβCD-treated monolayers were incubated with each chemical at 37°C for 30 minutes. Then free fluorescent markers were washed away, and monolayers were mounted on glass slides for confocal microscopy examination and quantitation of fluorescence intensity.

Imaging FRET measurements

Fluorescence microscopy was performed as described previously (Kenworthy and Edidin, 1998; Kenworthy and Edidin, 1999), with minor revisions. Cells were imaged on a Zeiss Axiovert 135TV microscope (Carl Zeiss, Thornwood, NY) using a 1.3 NA 100× Plan-neofluor objective. The digital images were collected using a 12-bit series 200 cooled charge-coupled device camera (Photometrics, Tuscon, AZ) operated using the IC300 digital imaging system (Inovision, Research Triangle Park, NC). Cy3 and Cy5 fluorescence was excited using a 75 W xenon arc lamp and detected using appropriate filter sets (Cy3 filter cube: excitation 515-560 nm, 565 nm long pass dichroic, emission 573-648 nm; Cy5 filter cube: excitation 590-650 nm, 660 nm long pass dichroic, emission 663-738 nm) (Chroma Technology, Brattleboro, VT). Images were collected with a Series 200 cooled CCD camera with a 1340×1037 pixel ICAF-1400 chip (Photometrics). Image acquisition time (less than 5 seconds) was adjusted to use the full linear intensity range of the CCD for each image. No fluorescence was observed from a Cy3-labeled specimen using the Cy5 filters, nor was Cy5 fluorescence detected using the Cy3 filter set.

In the present study, the acceptor bleaching FRET method was used, as described in detail (Kenworthy and Edidin, 1998; Kenworthy and Edidin, 1999). Briefly, the energy transfer was detected as an

increase in donor (Cy3) fluorescence (dequenching) after complete photobleaching of the acceptor (Cy5) fluorophore. The validity of using the acceptor photobleaching technique to quantify FRET depends on the fact that the only factor that can lead to a difference in donor fluorescence in the presence and absence of acceptor is energy transfer. Cells labeled only with Cy5-Stx1B were used to determine the minimum time required to completely bleach the Cy5. Typically, Cy5 was completely photobleached in 30 seconds of continuous arc lamp excitation using a Cy5 filter set. Under these conditions, ~97% of the Cy5 was bleached from the entire field of view, and no Cy3 bleaching or energy transfer occurred in control samples labeled with Cy3-CTB only (Fig. 2B,C). To perform an imaging FRET experiment, cells were stained with both Cy3-CTB and Cy5-Stx1B in the ratios 1:3 or 1:1. The image of Cy3-CTB (donor) in the presence of Cy5-Stx1B (acceptor) was obtained using a Cy3 filter set. Next, the image of Cy5-Stx1B was obtained using a Cy5 filter set. Then the same fluorescent field of view was continuously illuminated for 30 seconds at the Cy5 excitation wavelength and the image of Cy5 fluorescence after photobleaching was taken. Next another image of donor Cy3-CTB fluorescence was obtained using a Cy3 filter set. Images were collected from 6 to 10 different places from a single monolayer, stored on computer disk and fluorescence intensity of donor before and after acceptor photobleaching was measured for 50 identical 10×10 pixel regions of interest in each individual image using a custom-made program. FRET efficiency was calculated as:

$$E = (I_{D2} - I_{D1}) / I_{D2}$$

where I_{D1} and I_{D2} are the donor fluorescence intensities before and after acceptor photobleaching, respectively (Kenworthy and Edidin, 1997). FRET efficiency E was analyzed and plotted as a function of acceptor fluorescence intensity.

Stx1B binding/internalization analysis

To quantitate the total amount of fluorescent toxin that bound and was transported into the cells, monolayers, either unmodified (control) or modified by cholesterol-manipulating drugs, as described above, were incubated with Stx1B-OrG488 for 1 hour at 37°C and then free fluorescent toxin was washed away. To assay for binding without internalization, control and modified cells were stained with Stx1B-OrG488 for 1 hour at 4°C, washed with cold PBS and then fixed with paraformaldehyde for 1 hour at 4°C. Control and treated Caco-2 cells for each experiment were from the same passage with equal cell density to avoid artifacts related to the cell density and cell age.

To measure the amount of toxin associated with Caco-2 monolayers, two different techniques were applied: spectrofluorometry, which allowed collection of fluorescent signals from whole cell populations, and confocal microscopy, which allowed visualization of fluorescent toxin distribution on the cell surface and inside the cells and quantitation of the amount of fluorescent toxin from several regions of the monolayers.

In spectrofluorometer studies (SPF 500C, SML, Urbana, IL), control (n=4) and treated cells grown on glass coverslips were inserted in a spectrofluorometer chamber (n=4 in each treatment) and excited with 488 nm light. The emission spectra of Stx1B-OrG488 from 510 nm to 600 nm were collected from both control and treated monolayers. The photocounts in emission spectra represent only the amount of fluorescently labeled toxin bound to the cell surface or bound and internalized by cells. The intensity at the emission maximum (530 nm) from control monolayers, which corresponds to the amount of toxin, was quantitated as photocounts±s.e.m. and set at 100%±s.e.m. The amount of bound/transferred toxin in treated cells was calculated from the intensity at 530nm relative to the control.

In confocal microscopy studies, images were generated using the MRC 1024 MP system as described above. Optical sectioning from 15 different randomly chosen areas with multiple cells in each control (n=3) and experimental monolayer (n=3 for each type of treatment) were collected. Images were inclusively thresholded to eliminate background and ensure no pixels with intensity higher than 255 GL were included in analysis. The total fluorescence intensity in GL that corresponds to the amount of fluorescent Stx1B for each stack of images was measured (MetaMorph, Universal Imaging, West Chester, PA). The amount of bound/internalized toxin in control monolayers was calculated as mean GL±s.e.m and set at 100%±s.e.m. The amount of bound/internalized toxin in experimental monolayers was calculated as a percentage relative to the amount of total toxin in control cells.

To measure the amount of bound/internalized albumin or internalized 10K dextran in control and MβCD-treated cells, we use the confocal microscopy approach, as described above.

Statistics

Data are presented as mean±s.e.m. Significance was determined using the Student's t-test, and P values less than 0.05 were considered statistically significant.

RESULTS

Gb_3 is co-localized with G_{M1} on the apical surface of intestinal Caco-2 cells

It has been recently shown that the Stx1B receptor globotriaosylceramide Gb_3 is almost entirely localized in DIM in human renal tubular ACHN cells (Katagiri et al., 1999). Since Gb_3 receptors predominantly reside in LR, they were likely to co-localize with other glycosphingolipids, such as ganglioside G_{M1}, the CTB receptor that often serves as a LR marker (Abrami and van der Goot, 1999).

To study the distribution of Gb_3 on the apical surface of polarized Caco-2 cells with respect to LR, confluent monolayers were stained simultaneously with two different fluorescent markers, TMR-CTB, which specifically binds to ganglioside G_{M1}, and OrG488-Stx1B, which binds to Gb_3. Cells were incubated with both markers at a concentration of 1 μg/ml for 1 hour at 4°C to minimize endocytosis of the toxins. Confocal fluorescence images of confluent Caco-2 cells (Fig. 1) showed binding of both CTB and Stx1B and their co-localization on the apical surface. Analysis of six cells from

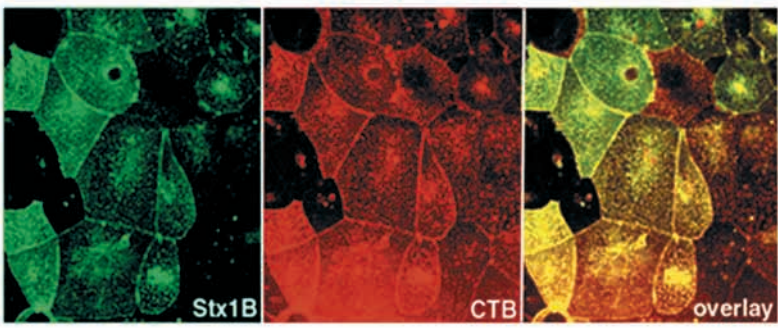

Fig. 1. Co-localization of Stx1B receptors and CTB receptors G_{M1} on the apical surface of Caco-2 intestinal epithelial cells. Confocal optical section through the apical surface of Caco-2 monolayers. Cells were double labeled with Stx1B-Oregon Green 488 (green) and CTB-TMR (red). Overlay panel shows co-localization of both receptors (yellow). Note, not all cells in confluent Caco-2 monolayers bind CTB and Stx1B due to the cell heterogeneity.

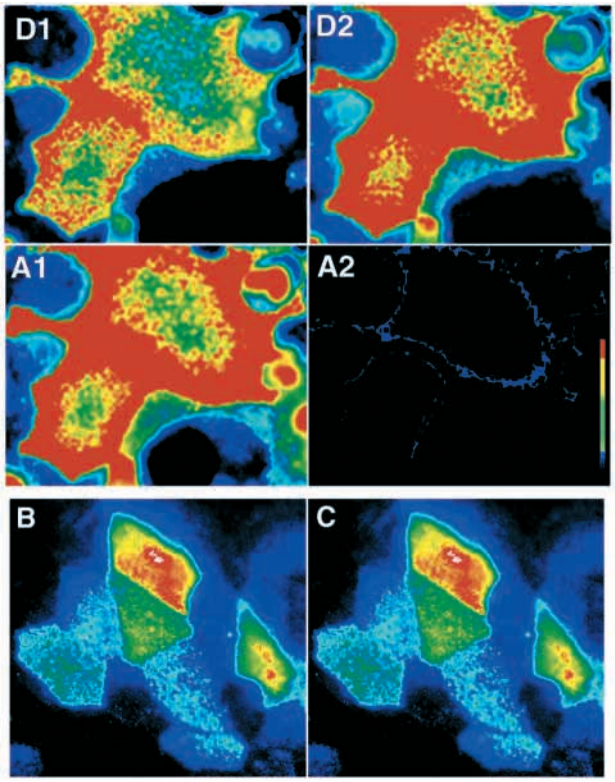

Fig. 2. Typical example of FRET between donor G_{M1} and acceptor Gb_3 molecules. (D1) Donor Cy3-CTB-G_{M1} image before acceptor photobleaching. (A1) Acceptor Cy5-Stx1B-Gb_3 image before photobleaching. (A2) Acceptor image after photobleaching. (D2) Donor image after acceptor photobleaching. Energy transfer can be detected from the increase in donor fluorescence (difference between D2 and D1 intensity fluorescence). In this experiment, the cells were labeled with donor- and acceptor-conjugated CTB and Stx1B at D:A=1:3 ratio. Colors reflect the fluorescence intensity of 8-bit images from lowest (black, 0 gray levels) to highest (red, 255 gray levels). The increase in D2 vs D1 fluorescence intensity is due to FRET. Note that neighboring cells, which are black on the D1 image because CTB intensity was below threshold level due to lower G_{M1} expression or due to a difference in cell thickness, appeared in blue color on the D2 image due to FRET. (B) Donor fluorescence intensity Cy3-CTB before and after (C) the bleaching period (30 seconds) in the absence of acceptor Cy5-Stx1B. Note that no donor bleaching or FRET occurred in that time period in the absence of acceptor.

two different preparations showed that ~97±6% of all labeled Gb_3 co-localized with labeled G_{M1}.

Recent data suggest that the LR in live cells are smaller than 70 nm in size (Varma and Mayor, 1998; Pralle et al., 2000). Based on co-localization results from confocal microscopy data (200 nm spatial resolution limitation), it is impossible to conclude that Gb_3 receptors reside in the same LR as G_{M1} molecules in living cell membranes. To examine the organization of Gb_3 molecules in intact cell membranes with high resolution, we applied the FRET method (Kenworthy and Edidin, 1998).

Gb_3 and G_{M1} molecules reside in the same LR

FRET was measured in terms of dequenching of donor fluorescence after complete photobleaching of the acceptor fluorophore as described above. Data from a typical imaging FRET experiment with D:A=1:3 are shown in Fig. 2. The initial Cy3-CTB image (Fig. 2D1) represents donor fluorescence in the presence of acceptor Cy5 (Fig. 2A1). After completely bleaching acceptor Cy5-Stx1B (Fig. 2A2), a second donor image was collected (Fig. 2D2). The fluorescence intensity of donor Cy3-CTB dramatically increased in all cells. Increased donor fluorescence after acceptor bleaching indicates that Cy3-CTB fluorescence was quenched in the presence of Cy5-Stx1B because of energy transfer.

The E% was calculated from the donor intensity before and after acceptor bleaching as described in the equation above. The calculated E for data shown in Fig. 2 was plotted against acceptor fluorescence (Fig. 3a). There was significant energy transfer between G_{M1} and Gb_3 molecules independent of acceptor concentration and E varied from region to region from 25% to 45% due to the difference in receptor expression on the apical surface of Caco-2 cells.

FRET theory predicts that, as well as being independent of acceptor concentration, E between clustered (linear relation between acceptor fluorescence and E) or partially clustered (hyperbolic relation between acceptor fluorescence and E) molecules is sensitive to the D:A ratio, while E between randomly distributed molecules is not sensitive to D:A and a plot of E vs acceptor fluorescence is identical for any given D:A ratio. We confirmed this by performing experiments with a ratio D:A=1:1, instead of 1:3. Again, we detected significant energy transfer, which was independent of acceptor concentration. However, FRET efficiency for D:A=1:1 was 10-20%, lower than FRET efficiency for D:A=1:3 (Fig. 3b). Thus, from imaging FRET we conclude that G_{M1} and Gb_3 receptor-ligand complexes are clustered in the same LR on the apical membrane of Caco-2 cells.

Caco-2 monolayers were treated with three different agents that sequester or deplete membrane cholesterol, a necessary LR component. These were: (1) mβCD, which extracts cholesterol from the membrane (Kilsdonk et al., 1995; Neufeld et al., 1996); (2) filipin, which binds to and sequesters cholesterol (Rothberg et al., 1990; Schnitzer et al., 1994); and (3) cholesterol oxidase (Okamoto et al., 2000). All of these agents disrupt G_{M1} and Gb_3 clustering. After treatment with all three agents, no FRET was detectable between Cy3-CTB and Cy5-Stx1B (Fig. 3c).

We also tested whether LR disruption changed the extent of co-localization between Gb_3 and G_{M1} molecules. We depleted cell cholesterol by treatment with MβCD. After exposure to MβCD, cells were fixed and incubated with both TMR-CTB and OrG488-Stx1B for 1 hour. Confocal images showed that both fluorescently labeled toxins bind to apical cell membrane with the same patchy pattern (Fig. 4A) as seen in control cells (Fig. 1); ~88±6% of Stx1B binding sites were co-localized with CTB binding sites (n=6 cells), an extent of co-localization not significantly different from non-treated cells (P=0.09).

Role of LR in Stx1B binding and translocation

LR may play an important role in Stx1B binding to the apical membrane of colonic cells because of the known high concentration of glycosphingolipids in rafts and because each subunit of the Stx1 B-pentamer attaches to three Gb_3 receptors (Ling et al., 1998). Based on our FRET data, Gb_3 receptors

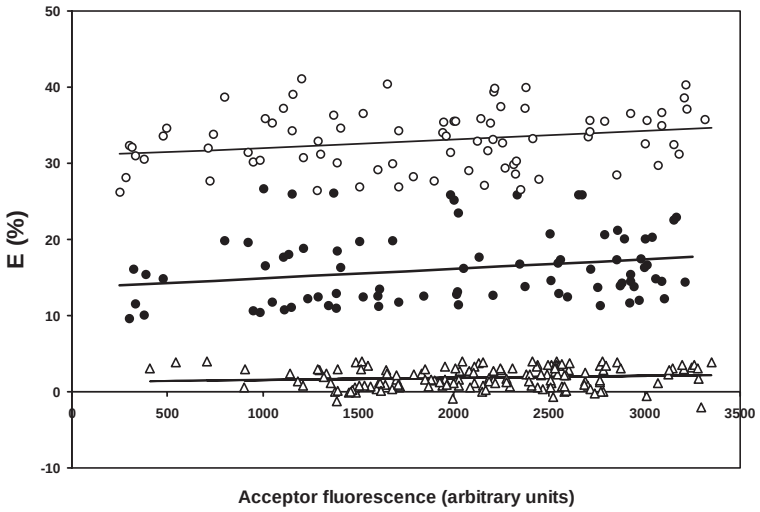

Fig. 3. Experimental FRET between donor G_{M1} and acceptor Gb_3 molecules. E increased as the concentration of acceptor Cy5-Stx1B used to label the cell was increased from D:A 1:1 (b, closed circles) to D:A 1:3 (a, open circles). In these experiments E increased from ~15% to ~33%, as D:A was increased. FRET does not occur between G_{M1} and Gb_3 molecules after MβCD treatment (c, open triangles).

reside in LR that are also enriched in G_{M1} and cholesterol. We speculated that disruption of LR integrity of Caco-2 cells would affect Stx1 binding and/or translocation.

Quantitation of the total amount of fluorescently labeled Stx1B by both spectrofluorometry and confocal microscopy gave similar results. All three agents that disrupted glycosphingolipid clusters significantly changed the amount of total bound and internalized toxin compared with control untreated monolayers with intact LR. Incubation of Caco-2 cells with mβCD reduced the total amount of toxin bound and accumulated inside the cells to 57±17% of control, filipin to 41±8% and cholesterol oxidase to 51±6% (Fig. 4B). The most aggressive method of cholesterol depletion, high concentration of MβCD, did not affect internalization of the fluid phase marker dextran (97±5% of control) and clathrin-mediated (Gekle et al., 1999) endocytosis of albumin (104±6% of control).

Cholesterol oxidase and MβCD did not affect Stx1B binding to the apical receptors. The amounts of bound fluorescent Stx1B were 97±3% of control in cholesterol oxidase-treated cells and 103±2% of control value in MβCD-treated cells (Fig. 4C). Exposure of cells to filipin slightly but significantly (Fig. 4C) increased Stx1-B binding to 115±2% (P<0.05).

DISCUSSION

The data presented here provide the first evidence that two different glycosphingolipids co-exist as receptor-ligand complexes in the same glycolipid-cholesterol microdomain or LR in vivo.

We used FRET microscopy to show that Stx1B-Gb_3 ligand-receptor complexes are (1) clustered rather than randomly distributed on apical membranes of living intestinal Caco-2 cells; and (2) are co-clustered with another glycosphingolipid, G_{M1}, which serves as the CT receptor (Fig. 2, Fig. 3). Because FRET imaging only reveals receptor-ligand complexes, it is possible, that distribution of empty receptors is different. However, it has been shown by FRET microscopy, that complexes of CT B-pentamer and G_{M1} are not clustered or only partially clustered (20%) in living cell membranes (Kenworthy and Edidin, 1998; Kenworthy et al., 2000).

Given that both Gb_3 and G_{M1} are bacterial toxin receptors, it is tempting to speculate that LR could have functional consequences as concentration sites for different kind of ligands. Recently, it has been shown that cholesterol-glycosphingolipid-rich microdomains act as concentration platforms for the pore-forming toxin aerolysin from *Aeromonas hydrophila* (Abrami and van der Goot, 1999). To test the possibility that Gb_3 molecules in cholesterol-enriched microdomains are necessary to increase the binding efficiency of Stx1B, we disrupted LR with three drugs that affect cholesterol differently. MβCD is a most effective extracellular cholesterol acceptor that extracts cholesterol from membranes (Kilsdonk et al., 1995). The polyene antibiotic filipin interacts with cholesterol and forms complexes in the plasma membrane (Schnitzer et al., 1994). Cholesterol oxidase converts cholesterol to cholestenone, an oxidation product of cholesterol (Okamoto et al., 2000). All of these agents, which disrupt LR, abolished FRET between labeled Gb_3 and labeled G_{M1}.

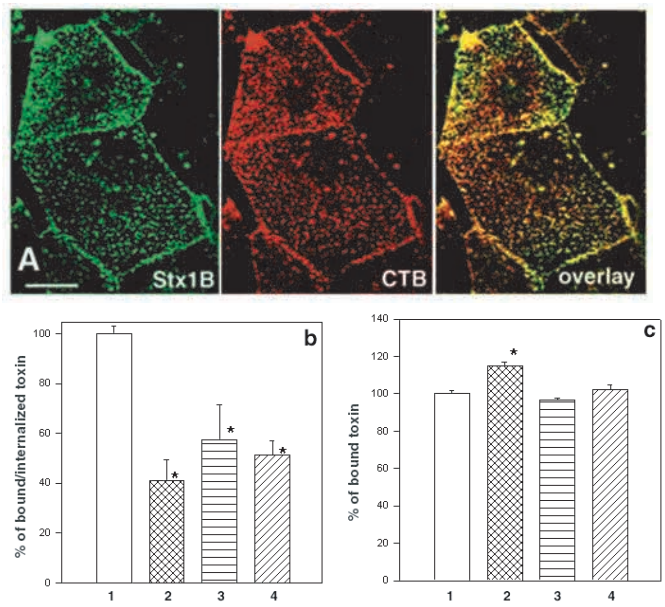

Fig. 4. Effect of cholesterol on Stx1B interaction with the apical surface of Caco-2 cells. (A) Stx1B and CTB co-localization in cells with disrupted LR. Confocal optical section through the apical surface of Caco-2 monolayers exposed to MβCD. Cells were double-labeled with Stx1B-Oregon Green 488 (green) and CTB-TMR (red). The overlay panel shows co-localization of both receptors (yellow). Bar, 5 μm. (B) Effect of cholesterol depletion on Stx1B binding plus internalization by Caco-2 cells. (C) effect of cholesterol depletion on Stx1B binding only by Caco-2 cells. (1) Control monolayers (n=7) with intact LR; (2) cells treated with filipin (n=7); (3) cells treated with MβCD (n=7); (4) cells incubated with cholesterol oxidase (n=7).

However, neither MβCD nor cholesterol oxidase treatment changed Stx1B binding to Gb_3 receptors (Fig. 4B). Cholesterol sequestration by filipin slightly but significantly increased the amount of Stx1B bound to its receptor. Similar results have been shown for CT binding to the apical membrane of Caco-2 cells, where 100 mg/ml 2-hydroxypropyl-β-cyclodextrin (2HO-βCD) had no effect on CTB binding to G_{M1} receptors. Exposure of monolayers to 1 μg/ml filipin slightly increased the amount of CT associated with the cell surface, probably due to the flattening of plasma membrane that may provide better access of the toxin to its receptor (Orlandi and Fishman, 1998). Moreover, it had been mentioned previously that Stx binding is unaffected by 10 mM MβCD in MDCK cells (Rodal et al., 1999).

The observation that depleting membrane cholesterol, thought to be essential for LR integrity does not affect binding of either Stx1B or CTB suggests to us that, at a constant level of receptor expression, toxin binding efficiency does not depend on clustered vs randomly distributed receptors. Moreover, it is unlikely that ligand binding caused receptor clustering. Rather, it indicates that empty Gb_3 and G_{M1} receptors themselves form a microdomain by interaction with cholesterol. Our results suggest that clustered toxin receptors function in toxin uptake.

After binding to Gb_3 receptors at 37°C, Stx1 is internalized by clathrin-dependent endocytosis (Sandvig and Van Deurs, 1996). Blocking clathrin-dependent endocytosis by cytosol acidification (Sandvig et al., 1989) or removal of clathrin-coated pits by potassium depletion (Sandvig and Van Deurs, 1994) prevents Stx1 entry and protects the cells from intoxication. Our study shows that the Stx1B internalization also depends on and is mediated through cholesterol-glycolipid-rich microdomains at the plasma membrane, similar to CTB endocytosis, where 1 μM filipin or 100 mg/ml 2HO-βCD significantly reduced the toxin internalization through caveolin or caveolae-like structures (Orlandi and Fishman, 1998).

There is growing evidence that cholesterol plays an important role in the endocytic pathway and that cholesterol depletion causes a functional perturbation of protein transport and endocytosis. Thus cholesterol is responsible for retention of GPI-anchored proteins in endosomes (Mayor et al., 1998). Lowering membrane cholesterol content inhibits receptor-mediated endocytosis of folate (Chang et al., 1992). Clathrin-dependent endocytosis is also sensitive to the removal of cholesterol by MβCD, which significantly reduces transferrin internalization (Rodal et al., 1999; Subtil et al., 1999). However, transferrin endocytosis is insensitive to filipin and cholesterol oxidase (Okamoto et al., 2000). By contrast, our data show that internalization of Stx1B is sensitive to both these agents as well as to MβCD. The decrease in Stx1B uptake caused by MβCD in our experiments was not due to cell damage, because fluid phase endocytosis of 10K dextran was similar to that in control cells. Surprisingly, the clathrin-mediated endocytosis of albumin (Gekle et al., 1999) was not significantly affected. Moreover, the same concentration of 2HO-βCD in 4 hours did not prevent the intoxification of Caco-2 cell by diphtheria toxin (Orlandi and Fishman, 1998). We found that the drugs, which differently affect different endocytic pathways, had the same effect on Stx1B internalization, inhibiting ~50% of toxin transfer across the membrane. Published data on CT translocation indicate that reducing membrane cholesterol affects the endocytosis of G_{M1}. Together, the data show that Gb_3 and G_{M1} glycosphingolipids are localized in the same microdomains, and their internalization requires intact microdomains. Recently it has been shown in MDCK cells that CTB and StxB share a common endocytic trafficking pathway, different from that for transferrin receptor internalization (Nichols et al., 2001). This pathway is highly sensitive to filipin, which reduced internalization of both CTB and StxB without a significant change in transferrin uptake. A higher filipin concentration (10 μM) than we used was needed to inhibit CT internalization in MDCK cells (Nichols et al., 2001). These differences may be related to cell line specificity, but, overall the data of Nichols et al. strongly support our finding that LR containing Gb_3 and G_{M1} play an important role in Stx1B uptake.

Disruption of LR structure by treatment of cells with cholesterol-affecting drugs could decrease the strength of interaction between the Stx1-Gb_3 complex and cholesterol and by that means influence the toxin endocytosis across the membrane.

Fusion of Gb_3-containing liposomes to the naturally toxin resistant, Gb_3-deficient CHO cells increased Stx1 binding but not cytotoxicity, showing that Gb_3 is required, but not sufficient for the action of Stx1 (Jacewicz et al., 1994). This result is in good agreement with our finding that separates toxin binding from uptake. Our results raise the possibility of the existence of a postbinding translocation mechanism linked to surface glycolipids and glycoproteins that does not exist in toxin-resistant cells or can be damaged by cholesterol depletion. Indeed, it has been recently shown that Stx binding caused the rapid temporary activation of Yes kinase (Katagiri et al., 1999). While the total amount of Yes per cell did not change, the amount of Yes in DIM increased after Stx treatment due to its association with Gb_3 molecules. However, in filipin-treated cells the amount of Yes in DIM was significantly reduced and Yes activation by Stx was dramatically suppressed. It is possible that removal of cholesterol changes the content of the Stx1B-Gb_3 translocation complex and/or interaction of other LR components within it that are necessary for toxin internalization.

We thank Drs A. Kane and D. W. K. Acheson from the New England Medical Center for supplying the purified Stx1B, and T. Pentcheva for technical assistance with FRET microscopy. This work was supported by the Hopkins Center for Epithelial Disorder, by grants from AHA 0160502U, NIH RO1 DK26523 and PO1 DK44484.

REFERENCES

Abrami, L. and van der Goot, F. G. (1999). Plasma membrane microdomains act as concentration platforms to facilitate intoxication by aerolysin. *J. Cell Biol.* **147**, 175-184.

Acheson, D. W. K. (1999). Foodborne infections. *Curr. Opin. Gasroent.* **15**, 538-545.

Acheson, D. W. K., Donohue-Rolfe, A. and Keusch, G. T. (1991). The family of Shiga and Shiga-like toxins. In *Sourcebook of Bacterial Protein Toxin* (ed. J. E. Aloufand and J. H. Freer), pp. 415-433, London, UK: Academic Press.

Acheson, D. W. K., Moore, R., DeBreucker, S., Lincicome, L., Jacewicz, M., Skutelsky, E. and Keusch, G. T. (1996). Translocation of Shiga toxin across polarized Intestinal cells in tissue culture *Infect. Immun.* **64**, 3294-3300.

Chang, W. J., Rothberg, K. G., Kamen, B. A. and Anderson, R. G. W. (1992). Lowering the cholesterol content of MAL04 cells inhibits receptor-mediated transport of folate. *J. Cell Biol.* **118**, 63-69.

Fuchs, G., Mobassaleh, M., Donohue-Rolfe, A., Montgomery, R. K., Grand, R. J. and Keusch, G. T. (1986). Pathogenesis of *Shigella diarrhea.* Rabbit intestinal cell microvillus membrane binding site for *Shigella* toxin. *Infect. Immun.* **53**, 372-377.

Gekle, M., Drumm, K., Mildenberger, S., Freudinger, R., Gassner, B. and Silbernagl, S. (1999). Inhibition of Na+-H+ exchange impairs receptor-mediated albumin endocytosis in renal proximal tubule-derived epithelial cells from opossum. *J. Physiol.* **520**, 709-721.

Jacewicz, M., Clausen, H., Nudelman, E., Donohue-Rolfe, A. and Keusch, G. T. (1986). Pathogenesis of *Shigella diarrhea*.11. Isolation of a *Shigella* toxin-binding glycolipid from rabbit jejunum and Hela cells and its identification as globotriaosylceramide. *J. Exp. Med*. **163**, 1391-1404.

Jacewicz, M. S., Mobassaleh, M., Gross, S. K., Balasubramanian, K. A., Daniel, P. F., Raghavan, S., McCluer, R. H. and Keusch, G. T. (1994). Pathogenesis of Shigella diarrhea:17. A mammalian-cell membrane glycolipid, Gb_3, is required but not sufficient to confer sensitivity to Shiga toxin. *J. Infect. Dis.* **169**, 538-546.

Jacobson, K. and Dietrich, C. (1999). Looking at lipid rafts? *Trends Cell Biol*. **9**, 87-91.

Katagiri, Y. U., Mori, T., Nakajima, H., Katagiri, C., Taguchi, T., Takeda, T., Kiyokawa, N and Fujimoto, J. (1999). Activation of Src family kinase Yes induced by Shiga toxin binding to globotriaosyl ceramide (/CD77) in low density, detergent-insoluble microdomains. *J. Biol. Chem*. **274**, 35278-35282.

Kenworthy, A. K. and Edidin, M. (1998). Distribution of glycosylphosphatidylinositol-anchored protein at the apical surface of MDCK cells examined at a resolution 100Å using imaging fluorescence resonance energy transfer. *J. Cell Biol*. **142**, 69-84.

Kenworthy, A. K. and Edidin, M. (1999) Imaging fluorescence resonance energy transfer as probe of membrane organization and molecular association of GPI-anchored proteins. *Methods Mol. Biol.* **116**, 37-49.

Kenworthy, A. K., Petranova, N. and Edidin, M. (2000). High-resolution FRET microscopy of cholera toxin B-subunit and GPI-anchored proteins in cell plasma membranes. *Mol. Biol. Cell* **11**, 1645-1655.

Kilsdonk, E. P., Yancey, P. G., Stoudt, G. W., Bangerter, F. W., Johnson, W. J., Phillips, M. C. and Rothblat, G. H. (1995). Cellular cholesterol efflux mediated by cyclodextrins. *J. Biol. Chem.* **270**, 17250-17256.

Lacy, D. B. and Stevens, R. (1998). Unraveling the structures and modes of action of bacterial toxins. *Curr. Opin. Struct. Biol*. **8**, 778-784.

Lindberg, C. A., Brown, J. E., Stromberg, N., Westling-Ryd, M., Schultz, J. E. and Karlson, K. (1987). Identification of the carbohydrate receptors for Shiga toxin produced by *Shigella dysenteriae* type1. *J. Biol. Chem.* **262**, 1779-1785.

Ling, H., Boodhoo, A., Hazes, B., Cummings, M. D., Armstrong, G. D., Brunton, J. L. and Read, R. J. (1998). Structure of the Shiga-like toxin I B-pentamer complexed with an analogue of its receptor. *Biochemistry* **37**, 1777-1788.

Mayor, S. and Maxfield, F. R. (1995). Insolubility and redistribution of GPI-anchored proteins at the cell surface after detergent treatment. *Mol. Biol. Cell.* **6**, 929-944.

Mayor, S., Sabharanjak, S. and Maxfield, F. R. (1998). Cholesterol-dependent retention of GPI-anchored proteins in endosomes. *EMBO J.* **17**, 4626-4638.

Neufeld, E. B., Cooney, A. M., Pitha, J., Dawidowicz, E. A., Dwyer, N. K., Pentchev, P. G. and Blanchette-Mackie, E. J. (1996). Intracellular trafficking of cholesterol monitored with a cyclodextrin. *J. Biol. Chem.* **271**, 21604-21613.

Nichols, B. J., Kenworthy, A. K., Polishchuk, R. S., Lodge, R., Roberts, T. H., Hirschberg, K., Phair, R. D. and Lippincott-Schwartz, J. (2001). Rapid cycling of lipid raft markers between the cell surface and Golgi complex. *J. Cell Biol.* **153**, 529-542.

Okamoto, Y., Ninomiya, H., Miwa, S. and Masaki, T. (2000). Cholesterol oxidation switches the internalization pathway of endothelin receptor type A from caveolae to clathrin-coated pits in CHO cells. *J. Biol. Chem.* **275**, 6439-6446.

Orlandi, P. A. and Fishman, P. H. (1998). Filipin-dependent inhibition of cholera toxin: evidence for toxin internalization and activation through caveolae-like domains. *J. Cell Biol.* **148**, 997-1007.

Pralle, A., Keller, P., Florin, E.-L., Simons, K. and Hörber, J. K. H. (2000). Sphingolipid-cholesterol rafts diffuse as small entities in the plasma membrane of mammalian cells. *J. Cell Biol.* **141**, 905-915.

Robson, W. L. M., Leung, A. K. C. and Montgomery, M. D. (1991). Causes of death in hemolytic uremic syndrome. *Child. Nephrol. Urol.* **11**, 228-233.

Rodal, S. K., Skretting, G., Garred, O., Vilhardt, F., van Deurs, B. and Sandvig, K. (1999). Extraction of cholesterol with methyl-β-cyclodextrin perturbs formation of clathrin-coated endocytic vesicles. *Mol. Biol. Cell* **10**, 961-974.

Rothberg, K. G., Ying, Y. S., Kolhouse, J. F., Kamen, B. A. and Anderson, R. G. W. (1990). The glycophospholipid-linked folate receptor internalizes folate without entering the clathrin-coated pit endocytic pathway. *J. Cell Biol*. **110**, 637-649.

Sandvig, K., Olsnes, S., Brown, J. E., Petersen, O. W. and Van Deurs, B. (1989). Endocytosis from coated pits of Shiga toxin: a glycolipid-binding protein from *Shigella dysenteriae* 1. *J. Cell Biol.* **108**, 1331-1343.

Sandvig, K. and Van Deurs, B. (1994). Entry of Shiga toxin into cells. *Zbl. Bakt.* **24**, 365-374.

Sandvig, K. and Van Deurs, B. (1996). Endocytosis, Intracellular transport, and cytotoxic action of Shiga toxin and ricin. *Physiol. Rev.* **76**, 949-966.

Schnitzer, J. E., Oh, P., Pinney, E. and Allard, J. (1994). Filipin-sensitive caveolae mediated transport in endothelium: reduced transcytosis, scavenger endocytosis and capillary permeability of select macromolecules. *J. Cell Biol.* **127**, 1217-1232.

St Hilaire, P. M., Boyd, M. K. and Toone, E. J. (1994). Interaction of the Shiga-like toxin type-1 b-subunit with its carbohydrate receptor. *Biochemistry* **33**, 14452-14463.

Subtil, A., Gaidarov, I., Kobylarz, K., Lampson, M. A., Keen, J. H. and McGraw, T. E. (1999). Acute cholesterol depletion inhibits clathrin-coated pit budding. *Proc. Natl. Acad. Sci. USA* **96**, 6775-6780.

Varma, R. and Mayor, S. (1998). GPI-anchored proteins are organized in submicron domains at the cell surface. *Nature* **394**, 798-801.

Wong, C. S., Jelacic, S., Habeeb, R. L., Watkins, S. L. and Tarr, P. I. (2000). The risk of the hemolytic-uremic syndrome after antibiotic treatment of *Escherichia coli* O157:H7 infections. *New Engl. J. Med.* **342**, 1930-1936.

Weinstein, D. L., Jackson, M. P., Perera, L. P., Holmes, R. K. and O'Brien, A. D. (1989). In vivo formation of hybrid toxins comprising Shiga toxin and the Shiga-like toxins and role of the b-subunit in localization and cytotoxic activity. *Infect. Immun.* **57**, 3743-3750.